
Graph Symbiosis Learning

Liang Zeng^{1*} Jin Xu^{1*} Zijun Yao² Yanqiao Zhu^{3,4} Jian Li¹

¹Institute for Interdisciplinary Information Sciences (IIIS), Tsinghua University

²Department of Computer Science and Technology, Tsinghua University

³Center for Research on Intelligent Perception and Computing
Institute of Automation, Chinese Academy of Sciences

⁴School of Artificial Intelligence, University of Chinese Academy of Sciences

{zengl18, j-xu18, yaozj20}@mails.tsinghua.edu.cn

yanqiao.zhu@cripac.ia.ac.cn

lijian83@mail.tsinghua.edu.cn

Abstract

We introduce a framework for learning from multiple generated graph views, named graph symbiosis learning (GraphSym). In GraphSym, graph neural networks (GNN) developed in multiple generated graph views can adaptively exchange parameters with each other and fuse information stored in linkage structures and node features. Specifically, we propose a novel adaptive exchange method to iteratively substitute redundant channels in the weight matrix of one GNN with informative channels of another GNN in a layer-by-layer manner. GraphSym does not rely on specific methods to generate multiple graph views and GNN architectures. Thus, existing GNNs can be seamlessly integrated into our framework. On 3 semi-supervised node classification datasets, GraphSym outperforms previous single-graph and multiple-graph GNNs without knowledge distillation, and achieves new state-of-the-art results. We also conduct a series of experiments on 15 public benchmarks, 8 popular GNN models, and 3 graph tasks—node classification, graph classification, and edge prediction—and show that GraphSym consistently achieves better performance than existing popular GNNs by 1.9%~3.9% on average and their ensembles. Extensive ablation studies and experiments on the few-shot setting also demonstrate the effectiveness of GraphSym.

1 Introduction

Graphs, composed of objects (*i.e.*, nodes) and their complex interactions (*i.e.*, edges), are widely used in modeling real-life applications, such as social networks, knowledge graphs, and biology networks [1–3]. In real-world scenarios, numerous systems are organized in the form of multiple graph views, where linkage structures and node features often convey information from multiple perspectives [3–7]. It is a common practice to construct multiple graph views generated from the original graph to provide complementary information of a graph [8–10]. Multiple generated graph views with different edge connections or node features contain rich information from different aspects, which is instrumental in our understanding of aggregating information from different generated graph views to learn better graph representations [5, 8, 10–17].

Recently, there are two main threads of research in multiple-graph GNNs¹. The first thread seeks to utilize graph augmentations to corrupt the positive samples to generate negative ones in contrastive learning on graphs [8, 11–14, 18], such as constructing graph views by dropping edges and masking

*Equal contribution.

¹In this paper, multiple-graph GNNs refer to GNNs trained on multiple generated graph views.

node features. The second aims to jointly model multiple graph views by co-regularization or architectural designs [10, 15–17, 19–24]. Both of them need specific domain knowledge to determine which sample is positive or design the network architecture and regularization term manually. In this work, we instead suppose that the integration of information from multiple generated graph views should not rely on specialized architectural designs or extra regularization terms, and powerful GNNs can first automatically and effectively learn the information from each single graph view and then exchange information with each other adaptively.

Symbiosis is a relationship between species living in a closely related environment, where participating species promote the fitness of each other by mutual interactions [25–27]. For example, the moth and the flower both live on the marshland. They benefit from each other by nectar collecting and pollination (as mutual interaction), and thus constitute a symbiosis relationship. GNNs are trained on multiple generated graph views, and are supposed to capture the graph information from different perspectives. Taking them as different species, one direction to promote their information fusion ability among multiple graphs is to mimic the mutual interaction and enable their symbiosis relationship, as shown in Figure 1. However, like the complex symbiosis relationship in biology, it is of vital importance to adaptively and effectively exchange parameters of GNNs trained on multiple generated graph views.

In this paper, we propose a novel framework for learning from multiple generated graph views, named graph symbiosis learning (GraphSym), which contains an individual phase and a symbiotic phase. In the individual phase, following previous work [9, 13, 14], we first leverage graph augmentations to automatically generate two views of a graph. Then, we develop two GNNs with the same architecture and each one is optimized by feeding a single-view graph. In the symbiotic phase, we quantitatively measure information of one layer in a GNN using entropy, and design a channel-wise adaptive exchange approach to replace redundant channels in one network with the informative channels from another network in a layer-by-layer manner. Furthermore, we extend to the multiple-graph GNNs case, where each GNN can contain information for all the other GNNs trained on multiple generated graph views.

The key contribution of this work is that we propose a novel graph symbiosis training framework that enables adaptive information exchange to effectively integrate knowledge from multiple generated graph views. GraphSym does not rely on specific methods to generate multiple graph views. Moreover, GraphSym does not need to modify the original training configurations such as learning rate, number of layers, and weight decay, requiring only information exchange in model parameters. Thus, existing GNN architectures can be seamlessly integrated into GraphSym. Furthermore, after exchanging parameters, there are no extra calculation overheads in the inference stage of GraphSym. On three semi-supervised node classification datasets, our method outperforms previous single-graph and multiple-graph GNNs that do not use knowledge distillation, and achieves new state-of-the-art results. We further evaluate the effectiveness of GraphSym on 15 public benchmark datasets, 8 popular GNN models, and 3 graph tasks such as node classification, edge prediction, and graph classification. GraphSym consistently outperforms baseline GNN models by 1.9%~3.9% (absolute improvements) on average on node classification, graph classification, and edge prediction tasks and their ensembles. In addition, our extensive ablation studies and analyses also demonstrate the superiority of GraphSym.

2 Related Work

Contrastive learning of multiple-graph GNNs. Contrastive learning is a discriminative approach by performing augmentations on a graph to obtain different views and maximizing the agreement of representations [28]. There is a large body of literature on contrastive multi-view representation

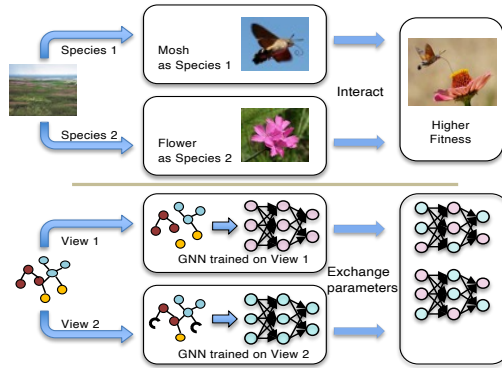


Figure 1: Symbiosis relationship in biology and multiple-graph GNNs. The moth and the flower are closely related due to the same living environment, whereas GNNs are trained with closely related views to the same graph. Ideally, multiple-graph GNNs benefit from mutual interactions of exchanging parameters, as it brings higher fitness to species with symbiotic interactions.

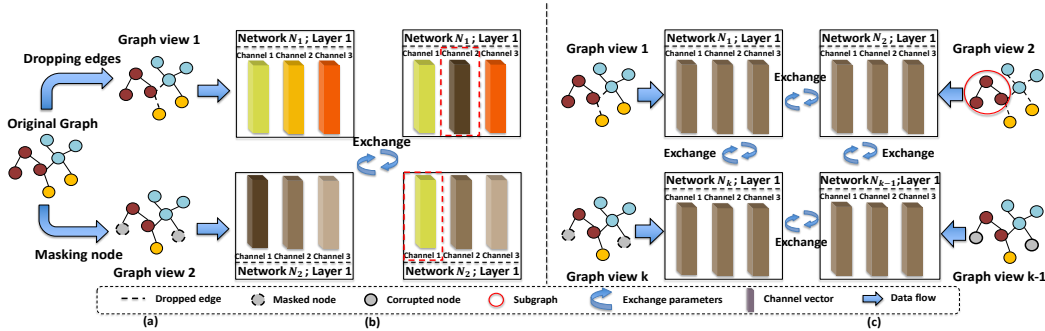


Figure 2: The illustrative schematic diagram of GraphSym. (a) Generating two graph views (*i.e.*, masking node features and dropping edges). (b) Adaptive channel-wise exchange (in the first layer for illustration). (c) GraphSym with multiple networks (best viewed in color).

learning in GNNs [8, 9, 11–14, 18, 29]. DGI [13] captures similarities using mutual information between node and graph summary vectors. GCA [9] uses an adaptive augmentation to generate informative views, which preserves important structural and attribute information of a graph. Although the approaches have achieved extensive success in various tasks, they need specialized graph augmentations to generate positive or negative samples. In contrast, our work can make use of broader augmentations and enable the exploitation of inner relationships of multiple generated graph views.

Joint learning of multiple-graph GNNs. Multiple-graph joint learning aims to jointly model multiple generated graph views to improve the generalization performance [10, 15–17, 19–24]. Most works leverage graph augmentations to generate multiple graph views from the original graph, and then design regularization term to force the GNN to optimize the prediction consistency or specialized architectures to directly model the relations between multiple graphs. Co-regularization based algorithms [10, 15, 19] regard the consistency of two graphs as a regularization term in the objective function. GRAND [10] designs a random propagation strategy to perform graph augmentations and utilizes consistency regularization to enforce the model to generate a similar feature map on different views of the same data. Besides, a number of architectural solutions have been proposed for joint learning of multiple-graph GNNs [16, 17, 20–24]. MGAT [16] explores an attention-based architecture to learn the node representation from multiple views of a graph. AM-GCN [24] proposes an adaptive multi-channel GNN and constructs two topology and feature graphs to integrate topological structures and node features. In contrast to these works, our work retains the benefits of joint modeling multiple generated graph views via symbiosis mechanism while not requiring extra regularization terms and specialized architectural designs.

Grafting. Grafting [30] inspires us to construct interaction with multiple networks. It improves the network performance by grafting external information (weights) on the same data source in computer vision tasks. Grafting calculates the weighted sum of parameters of two networks trained with different learning rates (hyper-parameters) to reactive invalid layers. It leverages layer-wise integration to achieve the best performance. In contrast, our work aims to adaptively integrate knowledge from GNNs trained on different generated graph views (data) to improve the generality of the model. Rather than using the weighted sum of parameters for the whole layer, we design a fine-grained approach to exchange part of the resource in each graph neural network by iteratively replacing redundant channels with informative channels in the weight matrix.

3 Methodology

In Section 3.1, we introduce the notations. In Section 3.2, we discuss the inspiration, and formulate the GraphSym framework. Next, we introduce GraphSym between two networks trained on two generated graph views, which can be divided into two phases: the individual phase (Section 3.3) and the symbiotic phase (Section 3.4). In section 3.5, we extend GraphSym to multiple GNNs.

3.1 Notations

Let $\mathcal{G} = (\mathcal{V}, \mathcal{E}, \mathbf{X})$ denote a graph, where \mathcal{V} is a set of $|\mathcal{V}| = n$ nodes, \mathcal{E} is a set of edges between nodes. $\mathbf{X} = [\mathbf{x}_1, \mathbf{x}_2, \dots, \mathbf{x}_n]^T \in \mathbb{R}^{n \times d}$ represents the node feature matrix and $\mathbf{x}_i \in \mathbb{R}^d$ is the feature vector of node v_i , where d is the channel of the feature matrix \mathbf{X} . The adjacency matrix $\mathbf{A} \in \{0, 1\}^{n \times n}$ is defined by $\mathbf{A}_{i,j} = 1$ if $(v_i, v_j) \in \mathcal{E}$, and 0 otherwise. A different view of the

original graph (\mathbf{X}, \mathbf{A}) is obtained by $(\widetilde{\mathbf{X}}, \widetilde{\mathbf{A}}) = \mathcal{C}(\mathbf{X}, \mathbf{A})$, where $\mathcal{C}(\cdot)$ is an *augmentation function*, such as masking node features and dropping edges [9, 13].

3.2 Inspiration & Formulation

Symbiosis is one of the common symbiotic relationships, in which organisms can promote each other to better adapt environment than those of living independently by exchanging resources or services [25–27]. Formally, we denote a parametrized GNN as $f_\theta : \mathbb{X} \rightarrow \mathbb{Y}$ with the initial parameter $\theta^{(0)}$, where \mathbb{X} and \mathbb{Y} are the input space and output space. In the individual phase, given M paired training data $\{(x_t, y_t)\}_{t=1}^M \subset \mathbb{X} \times \mathbb{Y}$, the network f_θ is optimized with a supervised loss \mathcal{L} as follows:

$$\theta^{(1)} = \arg \min_{\theta} \mathbb{E}_{(x,y) \in \mathbb{X} \times \mathbb{Y}} [\mathcal{L}(f_\theta(x), y)], \quad (1)$$

where $\theta^{(1)}$ is the weight of a GNN after optimization. Then, the symbiotic phase imitates the process of exchanging resources or services between two organisms in ecology. We take $\theta_1^{(1)}$ and $\theta_2^{(1)}$ of the two corresponding neural networks as input, exchange information, and produces $\theta_1'^{(1)}$ and $\theta_2'^{(1)}$ as output. At the final step, we re-train the output parameters $\theta_1'^{(1)}$ and $\theta_2'^{(1)}$ and get the final parameters $\theta_1^{(2)}$ and $\theta_2^{(2)}$. The illustration of the pipeline of parameter updating in GraphSym with two GNNs trained on two generated graph views is shown in Figure 3. We then proceed to introduce GraphSym in its two phases.

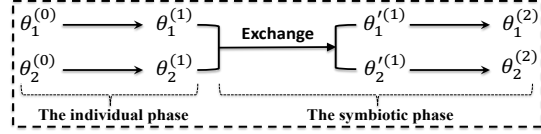


Figure 3: The illustration of the pipeline of parameter updating in GraphSym with two GNNs.

3.3 The Individual Phase

Generating multiple graph views. All organisms rely on their diverse environment to survive, such as sunlight and soil. In all these environments, organisms use available resources, interact and benefit from each other. To provide diverse environment for GNNs, following previous works [13, 9], we apply stochastic *augmentation functions* to generate multiple graph views and then feed them into GNNs. Once fitting these different generated graph views (environment), they can further improve performance by exchanging their knowledge. We leverage four augmentation functions to generate multiple graph views in symbiosis learning, which are *masking node features*, *corrupting node features*, *dropping edges*, and *extracting subgraphs*. The details of graph augmentations can be found in Appendix B. Note that GraphSym does not rely on specific methods to generate multiple graph views, thus other generating methods can be readily incorporated in our framework.

Training GNNs. GraphSym does not rely on specific GNN models and does not need to modify the original training configurations such as the number of layers and the learning rate. Thus, existing modern GNNs can be directly applied in our framework.

3.4 The Symbiotic Phase

After the individual phase, GNNs have learned the knowledge from multiple generated graph views and can take a further step to interact for mutual benefit. GNNs, developed from different views, should perform knowledge exchange with each other in a complementary way. To this end, we should first decide what information is valuable to exchange.

We use entropy to measure the information in one layer of a GNN. Let $\theta_{N_k}^i \in \mathbb{R}^{d_i \times d_{i+1}}$ be the weight of the i -th layer in GNN N_k , where d_i is the number of channels in the i -th layer. Following the previous approach introduced in [30–32], we calculate the entropy by dividing the range of values in $\theta_{N_k}^i$ into m different bins. Denote the number of values that fall into the i -th bin as n_i . We use $p_i \triangleq \frac{n_i}{(n_1 + \dots + n_m)}$ to approximate the probability of i -th bin, where $n_1 + \dots + n_m = d_i \times d_{i+1}$. Then, the entropy of $\theta_{N_k}^i$ can be calculated as follows:

$$H(\theta_{N_k}^i) = - \sum_{k=1}^m p_k \log p_k, \quad (2)$$

Algorithm 1: Graph symbiosis learning of two GNNs

- Input:** Two GNNs \mathcal{F}_1 and \mathcal{F}_2 , whose inputs are \mathcal{G}_1 and \mathcal{G}_2 , respectively; $\theta_k^{l,j} \in \mathbb{R}^{C_l \times C_{l+1}}$ denotes the weight of j -th channel in the l -th layer of network \mathcal{F}_k ; the number of layers of GNN L ; iteration number N ; the number of exchange channels M .
- 1 \triangleright **The individual phase:**
 - 2 Update the weights θ_1 of GNN $\mathcal{F}_1(\mathcal{G}_1; \theta_1)$ and θ_2 of GNN $\mathcal{F}_2(\mathcal{G}_2; \theta_2)$ according to the corresponding loss.
 - 3 \triangleright **The symbiotic phase:**
 - 4 Get the source and target GNN: $\mathcal{F}_{s\triangleleft} \leftarrow \mathcal{F}_1, \mathcal{F}_{t\triangleleft} \leftarrow \mathcal{F}_2$.
 - 5 **for** $n = 1 : N$ **do**
 - 6 **for** $l = 1 : L$ **do**
 - 7 Calculate the Pearson correlation among all possible pairs of the channels in $\theta_{t\triangleleft}^l$.
 - 8 Find a pair of channels indexed by idx_1 and idx_2 with the highest correlation.
 - 9 **for** $m = 1 : M$ **do**
 - 10 Substitute each channel of the source network $\theta_{s\triangleleft}^l$ for $\theta_{t\triangleleft}^{l,\text{idx}_1}$ or $\theta_{t\triangleleft}^{l,\text{idx}_2}$ of the target network to find an informative channel as Eq. 3.
 - 11 Reverse the source and target network $\mathcal{F}_{s\triangleright} \leftarrow \mathcal{F}_2, \mathcal{F}_{t\triangleright} \leftarrow \mathcal{F}_1$ and repeat the line 5-10.
 - 12 **Output** $\mathcal{F}_{t\triangleleft}$ and $\mathcal{F}_{t\triangleright}$.
-

A larger value of $H(\theta_{N_k}^i)$ indicates richer information in the weight of the i -th layer in GNN, and vice versa. For example, if each element of $\theta_{N_k}^i$ takes the same value (entropy is 0), $\theta_{N_k}^i$ cannot discriminate which part of the input is more important.

Adaptively exchange. Given the quantitative measurement of information in each layer of a GNN, we then consider how to exchange it in a complementary style. Thus we propose an adaptive exchange strategy to exchange the weights between two GNNs. GNNs follow the message passing framework to iteratively aggregate information from neighbor nodes. Specifically, the k -th layer makes use of the subtree structures of height k rooted at every node. Thus, we only exchange information of the same layer to preserve the consistency of information between two GNNs. Denote the weight in the l -th layer of a GNN trained on the k -th graph view as $\theta_k^l = [\theta_k^{l,1}, \dots, \theta_k^{l,C_{l+1}}] \in \mathbb{R}^{C_l \times C_{l+1}}$, where the input channel is C_l , the output channel is C_{l+1} and $\theta_k^{l,j} \in \mathbb{R}^{C_l}$ is an output channel vector. Denote the parameters of the source GNN as θ_s and the target GNN as θ_t . In each exchange step, our target is to adaptively exchange a channel in θ_t with another channel in θ_s for each layer. To substitute the redundant channel, we first calculate the Pearson correlation in θ_t^l and obtain a pair of redundant channels, *i.e.*, idx_1 and idx_2 , that have the highest correlation. Then we choose a channel from θ_s^l to maximize the entropy in the new weight matrix. Formally, let $f(\mathbf{A}, j, \mathbf{x})$ be the operation to substitute the j -th columns of the matrix \mathbf{A} with the vector \mathbf{x} . We find the informative channel $c \in [C_{l+1}]$ such that

$$\max_{\text{idx} \in \{\text{idx}_1, \text{idx}_2\}} H(f(\theta_t^l, \text{idx}, \theta_s^{l,c})) \quad (3)$$

is maximized. By repeating the above exchange step M times, θ_t^l can obtain the part of information (M channels) from θ_s^l while retaining the useful information in the original network. We also pictorially illustrate the procedure in Figure 2 (b). As we can see, GNN N_1 and N_2 perform adaptive channel-wise weight exchange in the first layer as aforementioned. As a result, N_1 substitutes the second channel in the weight matrix with the first channel in N_2 . Through this procedure, both networks contain information from two graph views. The complete algorithm is summarized in Algorithm 1. Finally, we re-train two GNNs with the same epochs introduced in Section 3.3 to obtain the output predictions.

3.5 Extending Symbiosis Learning to Multiple GNNs

Symbiosis learning can be easily extended to the case with multiple-graph GNNs, as illustrated in Figure 2 (c). In each iteration of the symbiotic phase, each network N_k receives the knowledge from N_{k-1} . After a certain iteration, each graph network contains the information for all the other

Table 1: Results of accuracy (%) on the Cora, Citeceer and Pubmed.

		Cora	CiteSeer	PubMed
Single-graph GNNs	GCN [33]	81.5	70.3	79.0
	GAT [34]	83.0±0.7	72.5±0.7	79.0±0.3
	GraphSAGE [35]	78.9±0.8	67.4±0.7	77.8±0.6
	APPNP [36]	83.8±0.3	71.6±0.5	79.7±0.3
	Graph U-Net [37]	84.4±0.6	73.2±0.5	79.6±0.2
	MixHop [38]	81.9±0.4	71.4±0.8	80.8±0.6
	SGC [39]	82.0±0.0	71.9±0.1	78.9±0.0
	GraphMix [40]	83.9±0.6	74.5±0.6	81.0±0.6
Multiple-graph GNNs	GCNII [41]	85.5±0.5	73.4±0.6	80.2±0.4
	MAGCN [22]	75.1	71.1	69.1
	DGI [13]	82.3±0.6	71.8±0.7	76.8±0.6
	GRAND [10]	85.4±0.4	75.5±0.4	82.7±0.6
Ours	Graft [30]	85.5±0.5	75.5±0.4	82.6±0.4
	Ensemble GraphSym	85.6 85.8±0.2	75.1 75.7±0.3	82.6 82.8±0.7

networks trained on multiple generated graph views. The complete algorithm of GraphSym with multiple-graph GNNs can be found in Appendix A.

4 Experiments

4.1 Setup

Dataset. Following previous multiple generated graph views learning approaches [8, 16, 10], we utilize single-view graphs datasets and generate multiple graph views via graph augmentations. To show the generality of the proposed GraphSym framework, we conduct experiments on 15 public benchmark datasets, including 9 datasets for *node classification*, 3 datasets for *edge prediction*, 5 datasets for *graph classification*, and 1 dataset for large scale node classification (*scalability*). Statistics of each dataset are summarized in Table 2 and Table 3. More details are included in Appendix D.

- **Node classification:** *Citation network* [42–44]: Cora, CiteSeer, and PubMed; *Wikipedia network* [45]: Chameleon, and Squirrel; *Actor co-occurrence network* [46]: Actor; *WebKB* [47]: Cornell, Texas, and Wisconsin.
- **Edge prediction:** *Citation network* [42–44]: Cora, CiteSeer, and PubMed.
- **Graph classification:** *Chemical compounds* [48]: DD, NCI1, and PROTEIN; *Social network* [48]: IMDB-BINARY and REDDIT-BINARY.
- **Scalability:** Academic citation network in the open graph benchmark (OGB) [49]: ogbn-arxiv.

Implementations. As a training scheme (rather than a specific GNN architecture), GraphSym is implemented *based on* a baseline GNN model by first training the GNN model on generated multiple graph views in the individual phase and then exchanging information among them in the symbiotic phase. For generating multiple views, we use *Masking node features*, *Corrupting node features*, *Drooping edges*, and *Extracting subgraphs* introduced in Appendix B as the graph augmentation methods. Data preparation follows the standard experimental settings, including feature preprocessing and data splitting. We conduct experiments on the transductive node, edge prediction [47, 33, 50] and inductive graph classification [51]. All the reported accuracy (%) are averaged over 100 runs, except 10 runs for the large-scale *ogbn-arxiv* dataset. Since each GNN in GraphSym interacts with all other GNNs, after symbiotic interaction, the performance of different GNNs is similar. Thus, in what follows, we always record the performance of the first GNN.

Baselines. To validate the effectiveness of our proposed method, we implement GraphSym based on the following GNN models²:

²We follow the settings in their original paper. The details refer to Appendix E.

Table 2: Results of accuracy (%) on node classification tasks. Δ denotes absolute differences between the original GCN and GraphSym. The average absolute improvements between each GNN model and GraphSym are presented in brackets.

	Cora	Citeseer	Pubmed	Chameleon	Squirrel	Actor	Cornell	Texas	Wisconsin
# Nodes: $ \mathcal{V} $	2,708	3,327	19,717	2,277	5,201	7,600	183	183	251
# Edges: $ \mathcal{E} $	5,278	4,676	44,327	31,421	198,493	26,752	280	295	466
# Features: d	1,433	3,703	500	2,325	2,089	931	1,703	1,703	1,703
# Classes: $ \mathcal{Y} $	7	6	3	5	5	5	5	5	5
GCN	81.2 \pm 0.6	70.4 \pm 0.9	78.7 \pm 0.5	53.0 \pm 2.4	36.8 \pm 1.7	27.6 \pm 1.3	53.3 \pm 3.2	58.8 \pm 4.9	51.9 \pm 6.8
+ FT	81.3 \pm 0.6	70.6 \pm 0.7	78.9 \pm 0.5	55.6 \pm 1.5	38.5 \pm 1.3	29.5 \pm 0.8	54.1 \pm 0.0	64.6 \pm 0.8	52.7 \pm 2.5
+ Ensemble	82.1 \pm 0.0	70.3 \pm 0.0	79.1 \pm 0.0	54.0 \pm 0.0	40.9 \pm 0.0	30.2 \pm 0.0	54.1 \pm 0.0	70.3 \pm 0.0	56.9 \pm 0.0
+ Ensemble + FT	81.6 \pm 0.4	70.0 \pm 0.3	79.5 \pm 0.5	56.2 \pm 0.8	40.9 \pm 0.2	30.6 \pm 0.5	54.1 \pm 0.0	66.5 \pm 1.8	56.9 \pm 1.2
+ GraphSym	82.5\pm0.3	70.7\pm0.3	79.6\pm0.1	57.1\pm0.9	41.4\pm0.1	31.0\pm0.4	54.1\pm0.0	71.8\pm2.0	57.5\pm0.9
Δ (3.8)	1.3\uparrow	0.3\uparrow	0.9\uparrow	4.1\uparrow	4.6\uparrow	3.4\uparrow	0.8\uparrow	13.0\uparrow	5.6\uparrow
GAT	82.7 \pm 0.4	70.0 \pm 0.6	78.3 \pm 0.6	55.5 \pm 1.3	30.1 \pm 2.3	26.0 \pm 0.5	52.0 \pm 2.4	64.4 \pm 1.7	53.4 \pm 2.6
+ FT	82.1 \pm 0.6	69.9 \pm 0.7	77.8 \pm 0.8	55.8 \pm 1.7	30.6 \pm 1.5	30.6 \pm 1.5	51.9 \pm 2.0	63.2 \pm 2.8	53.9 \pm 2.2
+ Ensemble	81.7 \pm 0.0	69.3 \pm 0.0	78.5 \pm 0.0	54.6 \pm 0.0	32.0 \pm 0.0	32.0 \pm 0.0	54.1 \pm 0.0	64.9 \pm 0.0	56.9 \pm 0.0
+ Ensemble + FT	82.7 \pm 0.3	69.2 \pm 0.4	78.4 \pm 0.2	56.8 \pm 0.5	31.5 \pm 0.8	31.5 \pm 0.8	49.2 \pm 1.1	62.2 \pm 0.0	53.9 \pm 1.8
+ GraphSym	83.1\pm0.2	70.1\pm0.3	78.6\pm0.3	56.7\pm1.4	32.5\pm0.2	32.5\pm0.2	54.1\pm0.1	64.9\pm0.0	56.9\pm1.6
Δ (1.9)	0.4\uparrow	0.1\uparrow	0.3\uparrow	1.2\uparrow	2.4\uparrow	6.5\uparrow	2.1\uparrow	0.5\uparrow	3.5\uparrow
APPNP	82.0 \pm 1.1	70.4 \pm 1.1	79.2 \pm 0.9	47.7 \pm 2.7	28.4 \pm 2.4	31.8 \pm 1.7	50.4 \pm 2.8	63.3 \pm 2.5	49.8 \pm 3.1
+ FT	81.9 \pm 1.1	70.7 \pm 1.0	79.1 \pm 0.8	49.1 \pm 1.7	28.7 \pm 2.0	31.3 \pm 2.0	49.7 \pm 2.8	62.8 \pm 2.2	51.2 \pm 3.8
+ Ensemble	82.0 \pm 0.0	69.5 \pm 0.0	78.8 \pm 0.0	51.1 \pm 0.0	26.9 \pm 0.0	32.9 \pm 0.0	54.1 \pm 0.0	64.9 \pm 0.0	56.8 \pm 0.0
+ Ensemble + FT	82.3 \pm 0.7	69.4 \pm 1.3	79.7 \pm 0.5	51.7 \pm 1.5	31.4 \pm 0.8	32.1 \pm 0.8	50.0 \pm 1.8	56.8 \pm 1.9	51.0 \pm 1.2
+ GraphSym	82.7\pm0.2	71.0\pm0.2	79.7\pm0.1	52.6\pm0.1	31.6\pm1.3	33.3\pm0.1	55.4\pm1.4	68.5\pm1.3	56.9\pm0.1
Δ (3.2)	0.7\uparrow	0.6\uparrow	0.5\uparrow	4.9\uparrow	3.2\uparrow	1.5\uparrow	5.0\uparrow	5.2\uparrow	7.1\uparrow
JKNET-CAT	81.9 \pm 0.5	69.2 \pm 0.5	78.3 \pm 0.2	55.7 \pm 2.2	36.4 \pm 1.7	28.5 \pm 1.3	53.9 \pm 4.7	59.5 \pm 5.1	51.5 \pm 5.4
+ FT	81.3 \pm 0.4	68.1 \pm 1.0	77.8 \pm 0.6	56.9 \pm 1.4	36.1 \pm 0.9	28.3 \pm 0.5	52.7 \pm 2.5	61.9 \pm 0.8	51.4 \pm 2.1
+ Ensemble	82.0 \pm 0.0	67.2 \pm 0.0	77.6 \pm 0.0	58.1 \pm 0.0	36.6 \pm 0.0	29.5 \pm 0.0	54.1 \pm 0.0	67.6 \pm 0.0	56.9 \pm 0.0
+ Ensemble + FT	82.0 \pm 0.3	67.6 \pm 0.5	78.1 \pm 0.3	57.7 \pm 0.8	36.3 \pm 0.5	29.1 \pm 0.5	47.8 \pm 2.5	67.6 \pm 0.0	52.5 \pm 1.5
+ GraphSym	82.4\pm0.2	69.5\pm0.1	78.5\pm0.1	59.4\pm0.1	37.0\pm0.3	29.6\pm0.4	54.2\pm0.1	67.6\pm0.0	56.9\pm0.0
Δ (3.2)	0.5\uparrow	0.3\uparrow	0.2\uparrow	3.7\uparrow	0.6\uparrow	1.0\uparrow	0.3\uparrow	8.1\uparrow	5.4\uparrow
JKNET-MAX	81.9 \pm 0.7	69.2 \pm 0.1	78.4 \pm 0.2	54.8 \pm 2.1	36.0 \pm 1.9	28.3 \pm 1.5	52.2 \pm 3.4	60.1 \pm 5.1	52.0 \pm 5.5
+ FT	81.3 \pm 0.6	68.3 \pm 1.3	77.7 \pm 0.5	56.2 \pm 1.0	36.1 \pm 0.9	27.9 \pm 0.5	53.5 \pm 1.0	64.1 \pm 1.9	53.1 \pm 2.2
+ Ensemble	81.4 \pm 0.0	67.1 \pm 0.0	77.2 \pm 0.0	55.7 \pm 0.0	37.4 \pm 0.0	26.6 \pm 0.0	54.1 \pm 0.0	70.1 \pm 0.0	56.9 \pm 0.0
+ Ensemble + FT	82.3 \pm 0.2	67.7 \pm 0.5	77.8 \pm 0.3	54.6 \pm 1.0	36.4 \pm 0.5	28.0 \pm 0.5	54.1 \pm 0.0	66.9 \pm 1.2	55.3 \pm 0.8
+ GraphSym	82.4\pm0.2	69.5\pm0.1	78.6\pm0.1	57.4\pm0.3	37.7\pm0.2	28.9\pm0.2	54.1\pm0.0	70.3\pm1.5	57.6\pm1.0
Δ (2.2)	0.5\uparrow	0.3\uparrow	0.2\uparrow	2.6\uparrow	1.7\uparrow	0.6\uparrow	1.9\uparrow	10.2\uparrow	5.6\uparrow
GCNII	85.2 \pm 0.4	73.2 \pm 0.5	80.0 \pm 0.3	60.7 \pm 2.1	44.1 \pm 1.9	30.1 \pm 0.9	61.2 \pm 2.1	67.0 \pm 6.3	74.7 \pm 3.4
+ FT	84.6 \pm 0.6	72.1 \pm 0.8	77.7 \pm 0.8	61.9 \pm 1.6	45.0 \pm 0.9	30.0 \pm 0.6	60.9 \pm 2.5	68.6 \pm 1.8	72.7 \pm 3.4
+ Ensemble	85.1 \pm 0.0	72.4 \pm 0.0	78.4 \pm 0.0	62.9 \pm 0.0	43.8 \pm 0.0	30.3 \pm 0.0	59.5 \pm 0.0	78.4 \pm 0.0	72.6 \pm 0.0
+ Ensemble + FT	85.3 \pm 0.3	71.6 \pm 0.7	78.8 \pm 0.9	62.4 \pm 1.3	45.7 \pm 0.4	30.3 \pm 0.4	60.0 \pm 2.0	76.2 \pm 2.0	71.6 \pm 3.3
+ GraphSym	85.6\pm0.2	73.5\pm0.1	80.2\pm0.1	63.1\pm1.3	46.0\pm0.7	31.4\pm0.1	62.8\pm1.2	79.7\pm2.8	76.8\pm1.9
Δ (2.6)	0.4\uparrow	0.3\uparrow	0.2\uparrow	2.4\uparrow	1.9\uparrow	1.3\uparrow	1.6\uparrow	12.7\uparrow	2.1\uparrow

- **Node classification:** GCN [33], GAT [34], APPNP [36], JKNET with concatenation and maximum aggregation scheme [52], GRAND [10], and a recent deep GCN model GCNII [41].
- **Edge prediction:** GCN [33].
- **Graph classification:** GCN [33], and GIN [53].

Besides, we test 3 variants for each GNN model for ablation analysis. To exclude the influence of longer training epochs, we conduct experiments, named further training (**FT**), to train the baseline models with the same number of epochs as GraphSym. Multiple-graph GNNs ensemble (**Ensemble**) first trains each GNN on the individual generated view of a graph and then assemble their outputs by majority voting. Multiple-graph GNNs ensemble+further training (**Ensemble+FT**) is similar to Ensemble but trains each GNN with the same number of epochs as GraphSym. The original GNN models of the baselines are denoted by their name directly.

Table 3: Results of accuracy (%) on graph classification tasks. We leverage model selection strategies and data splits following [51].

	DD	NCII	PROTEINS	IMDB-BINARY	REDDIT-BINARY
# Graphs: $ \mathcal{G} $	1,178	4,110	1,113	1,000	2,000
# Average nodes: $ \mathcal{V} / \mathcal{G} $	284.32	29.87	39.06	19.77	429.63
# Average edges: $ \mathcal{E} / \mathcal{G} $	715.66	32.30	72.82	96.53	497.75
# Labels: $ \mathcal{L} $	2	2	2	2	2
GCN	76.5 \pm 3.0	76.3 \pm 1.4	73.3 \pm 3.9	70.5 \pm 4.5	88.6 \pm 2.3
+ FT	76.4 \pm 3.6	73.8 \pm 2.3	71.1 \pm 3.6	68.5 \pm 4.6	88.4 \pm 2.3
+ Ensemble	80.5 \pm 2.5	80.5 \pm 1.2	78.9 \pm 3.2	54.8 \pm 4.3	81.5 \pm 3.1
+ Ensemble + FT	79.6 \pm 4.1	81.1 \pm 2.1	74.5 \pm 4.0	68.1 \pm 4.7	87.2 \pm 2.8
+ GraphSym	81.0\pm3.4	81.5\pm2.4	80.4\pm3.5	72.4\pm2.4	89.5\pm1.9
Δ (3.9)	4.5 \uparrow	5.2 \uparrow	7.1 \uparrow	1.9 \uparrow	0.9 \uparrow
GIN	75.7 \pm 1.1	79.0 \pm 1.5	73.7 \pm 3.6	71.7 \pm 5.9	89.0 \pm 2.5
+ FT	69.2 \pm 3.3	74.1 \pm 4.0	66.3 \pm 4.3	58.5 \pm 7.5	81.1 \pm 10.3
+ Ensemble	82.1 \pm 1.9	79.5 \pm 1.6	75.8 \pm 3.3	71.5 \pm 4.4	49.7 \pm 3.6
+ Ensemble + FT	81.0 \pm 3.5	79.8 \pm 2.0	70.7 \pm 4.3	63.5 \pm 5.6	88.7 \pm 4.4
+ GraphSym	82.2\pm1.2	79.8\pm2.0	76.8\pm2.0	72.3\pm6.3	90.6\pm1.4
Δ (2.5)	6.5 \uparrow	0.8 \uparrow	3.1 \uparrow	0.6 \uparrow	1.6 \uparrow

Table 4: Results of accuracy (%) on edge prediction tasks.

Dataset	GCN	FT	Ensemble	Ensemble + FT	GraphSym	Δ (2.9)
Cora	90.3 \pm 1.2	91.6 \pm 0.9	93.8 \pm 0.6	94.3 \pm 0.7	94.6\pm0.8	4.3 \uparrow
CiteSeer	89.1 \pm 1.3	89.8 \pm 0.8	92.3 \pm 0.7	92.1 \pm 0.6	92.6\pm0.4	3.5 \uparrow
PubMed	95.4 \pm 0.3	95.6 \pm 0.2	95.3 \pm 0.2	96.1 \pm 0.2	96.2\pm0.2	0.8 \uparrow

4.2 Experimental Results

Node classification. We implement Ensemble and GraphSym based on GRAND [10]. The comparison with the baselines on Cora, CiteSeer, and PubMed datasets is reported in Table 1. We can see that GraphSym achieves state-of-the-art results among both the single-graph GNNs and multiple-graph GNNs, which demonstrates the effectiveness of symbiosis learning in modeling the relationship of multiple generated graph views. The outperformance over the Ensemble shows that the adaptive integration of multiple generated graph views in our symbiosis learning is superior to the simple integration of multiple-graph GNNs. In contrast to Ensemble, which requires the simultaneous inference of multiple models, the inference cost of GraphSym is the same as a single-graph model. Moreover, we compare our methods with Graft [30] by replacing our adaptive exchange scheme with the adaptive weighting method. We can find that our method consistently surpasses Graft, which suggests that our fine-grained approach to exchange part of resource in each GNN is a more effective approach for multiple-graph GNNs.

To further evaluate the effectiveness of GraphSym, we implement GraphSym and compare it with the 3 variants of the baseline GNN model. The baseline models include GCN, GAT, APPNP, JKNet, and GCNII [33, 34, 36, 52, 41]. The results of baselines are reproduced based on their official codes. Experimental results are reported in Table 2. It is shown that GraphSym consistently outperforms baselines by 1.9%~3.8% (absolute improvements) on average. The outperformance of GraphSym over FT, Ensemble, and Ensemble+FT shows that the expressiveness of the symbiosis learning comes from neither extra training epochs, nor the larger model capacity of multiple-graph GNNs. Besides, in contrast to the ensemble methods, GraphSym utilizes only one network during inference, which is more computationally efficient.

Table 5: Results of accuracy (%) on ogbn-arxiv .

ogbn-Arxiv	GCNII	GCN_res-v2	GCN_DGL	GraphSAGE
Original	72.7 \pm 0.2	71.5 \pm 0.9	70.9 \pm 0.5	71.5 \pm 0.4
+ FT	71.8 \pm 0.5	71.5 \pm 0.8	71.1 \pm 0.4	OOM
+ Ensemble	71.5 \pm 0.0	71.9 \pm 0.0	70.4 \pm 0.0	71.4 \pm 0.0
+ Ensemble + FT	72.4 \pm 0.3	72.0 \pm 0.4	70.9 \pm 0.2	OOM
+ GraphSym	72.9\pm0.5	72.1\pm0.6	71.5\pm0.7	71.9\pm0.2
Δ (0.5)	0.2 \uparrow	0.6 \uparrow	0.6 \uparrow	0.4 \uparrow

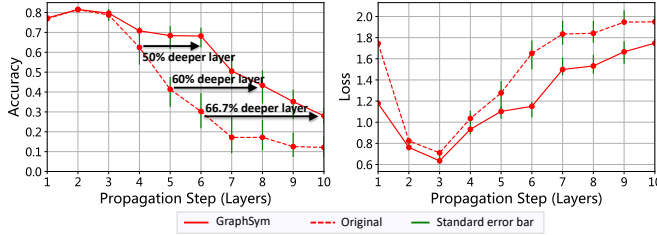


Figure 4: Training curves on Cora.

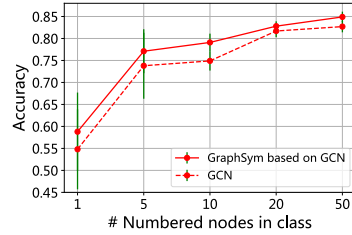


Figure 5: Few-shot learning on Cora.

Edge prediction and graph classification. To investigate the generality of GraphSym, we further conduct experiments on two common graph tasks: edge prediction and graph classification. As shown in Table 4 and 3, GraphSym consistently outperforms the original GNN model by a large margin. Meanwhile, GraphSym achieves a higher accuracy over the 3 variants, further showing that adaptively exchanging parameters among multiple generated graph views is more effective than model ensemble.

Scalability. To show the scalability of GraphSym, we conduct experiments on the large citation dataset *ogbn-arxiv*. We select four top-ranked GNN models from the leader-board of OGB, and then perform GraphSym based on them with the same GNN architectures and hyperparameters (see Appendix E for more details). As shown in Table 5, our method outperforms the original methods and their ensembles, which demonstrates the scalability of GraphSym.

4.3 Experimental Analysis

Over-smoothing. GNNs are shown to suffer from the over-smoothing issue, where node features become indistinguishable as we increase the feature propagation steps [54–56]. Thus, it is difficult to extend model capacity for large-scale graphs by deepening GNNs. We represent the results of GCN [33] by increasing the propagation steps (layers) and implement GraphSym based on GCN for comparison. As shown in Figure 4, we empirically find that GraphSym can mitigate the over-smoothing issue compared to the original GCN. As the number of layers increases, the accuracy of the original GNN decreases dramatically—from 0.8 to 0.1. In contrast, the accuracy of GraphSym decreases much slower. This suggests that GraphSym provides a principled way to extend model capacity with relatively large layer numbers due to the adaptive information exchange scheme.

Few-shot. We further evaluate the effectiveness of GraphSym under few-shot settings. Taking the Cora as the representative dataset, we manually vary the number of training nodes per class from 1 to 50, and keep the validation and test dataset unchanged. As shown in Figure 5, GraphSym consistently outperforms GCN. Specifically, the relative improvements on classification accuracy are 4.0/3.3/4.2/0.9/2.2 on average for 1/5/10/20/50 labeled nodes per class, which shows that integrating information from multiple generated graph views is more efficient in utilizing limited supervision.

Hyperparameter study. We study the effects of hyperparameters of our framework GraphSym, and conduct experiments on Cora based on the GCN model. We have two hyperparameters in the symbiotic phase: the iteration number N and the exchanging channels M . Taking the GraphSym on 4 graph views as an example, we first present a study on the iteration number

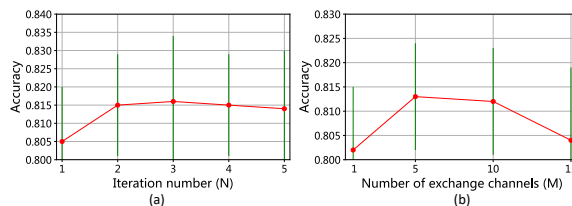


Figure 6: Hyper-parameter study on Cora.

by varying N from 1 to 5 while using default value $M = 5$. As shown in Figure 6 (a), our proposed framework achieves relatively stable performance. We further study the number of exchange channels M by varying it from 1 to 15 (the hidden size of the GCN is 16) while fixing $N = 2$. The best performance is achieved by exchanging part of channels rather than all weights in a layer, demonstrating that adaptively exchanging information in a complementary way can bring more benefits. In all, we can find that the performance of our framework is relatively stable across different hyperparameters and thus does not rely on heavy and case-by-case hyperparameter tuning to achieve the best results.

5 Conclusion

In this paper, we propose a new framework on multiple generated graph views, named graph symbiosis learning (GraphSym). In GraphSym, we propose a novel adaptive exchange method to iteratively substitute the redundant channels in the weight matrix of one GNN with informative channels of another GNN in a layer-by-layer manner. GraphSym does not rely on GNN architectures and specific methods to generate multiple graph views. Thus, existing GNNs can be readily integrated into our framework. Comprehensive experiments on real datasets show that our proposed training framework outperforms the existing popular GNNs models and their ensembles. For future work, we will utilize more adaptive graph augmentations to further improve the performance of GraphSym. We hope our work will inspire new ideas in exploring new training mechanisms on multiple-graph GNNs.

References

- [1] David Easley and Jon Kleinberg. *Networks, Crowds, and Markets - Reasoning About a Highly Connected World*. Cambridge university press Cambridge, 2010.
- [2] Albert-László Barabási. Network science. *Philosophical Transactions of the Royal Society A: Mathematical, Physical and Engineering Sciences*, 371(1987):20120375, 2013.
- [3] William L Hamilton. Graph representation learning. *Synthesis Lectures on Artificial Intelligence and Machine Learning*, 14(3):1–159, 2020.
- [4] Peter W Battaglia, Jessica B Hamrick, Victor Bapst, Alvaro Sanchez-Gonzalez, Vinicius Zambaldi, Mateusz Malinowski, Andrea Tacchetti, David Raposo, Adam Santoro, and Ryan Faulkner. Relational inductive biases, deep learning, and graph networks. *arXiv preprint arXiv:1806.01261*, 2018.
- [5] Baoyu Jing, Chanyoung Park, and Hanghang Tong. Hdmi: High-order deep multiplex infomax. *arXiv preprint arXiv:2102.07810*, 2021.
- [6] Zonghan Wu, Shirui Pan, Fengwen Chen, Guodong Long, Chengqi Zhang, and S Yu Philip. A comprehensive survey on graph neural networks. *IEEE transactions on neural networks and learning systems*, 2020.
- [7] Youwei Liang, Dong Huang, Chang-Dong Wang, and Philip S Yu. Multi-view graph learning by joint modeling of consistency and inconsistency. *arXiv preprint arXiv:2008.10208*, 2020.
- [8] Kaveh Hassani and Amir Hosein Khasahmadi. Contrastive multi-view representation learning on graphs. In *International Conference on Machine Learning*, pages 4116–4126. PMLR, 2020.
- [9] Yanqiao Zhu, Yichen Xu, Feng Yu, Qiang Liu, Shu Wu, and Liang Wang. Graph contrastive learning with adaptive augmentation. *arXiv preprint arXiv:2010.14945*, 2020.
- [10] Wenzheng Feng, Jie Zhang, Yuxiao Dong, Yu Han, Huanbo Luan, Qian Xu, Qiang Yang, Evgeny Kharlamov, and Jie Tang. Graph random neural networks for semi-supervised learning on graphs. *Advances in Neural Information Processing Systems*, 33, 2020.
- [11] Yuning You, Tianlong Chen, Yongduo Sui, Ting Chen, Zhangyang Wang, and Yang Shen. Graph contrastive learning with augmentations. In *Advances in neural information processing systems*, 2020.
- [12] Ben Poole, Sherjil Ozair, Aaron Van Den Oord, Alex Alemi, and George Tucker. On variational bounds of mutual information. In *International Conference on Machine Learning*, pages 5171–5180. PMLR, 2019.
- [13] Petar Veličković, William Fedus, William L Hamilton, Pietro Liò, Yoshua Bengio, and R Devon Hjelm. Deep graph infomax. In *Proceedings of the International Conference on Learning Representations (ICLR)*, 2018.
- [14] Fan-Yun Sun, Jordan Hoffmann, Vikas Verma, and Jian Tang. Infograph: Unsupervised and semi-supervised graph-level representation learning via mutual information maximization. In *Proceedings of the International Conference on Learning Representations (ICLR)*, 2020.

- [15] Shaohua Fan, Xiao Wang, Chuan Shi, Emiao Lu, Ken Lin, and Bai Wang. One2multi graph autoencoder for multi-view graph clustering. In *Proceedings of The Web Conference 2020*, pages 3070–3076, 2020.
- [16] Yu Xie, Yuanqiao Zhang, Maoguo Gong, Zedong Tang, and Chao Han. Mgat: Multi-view graph attention networks. *Neural Networks*, 132:180–189, 2020.
- [17] Hehuan Ma, Yatao Bian, Yu Rong, Wenbing Huang, Tingyang Xu, Weiyang Xie, Geyan Ye, and Junzhou Huang. Multi-view graph neural networks for molecular property prediction. *arXiv preprint arXiv:2005.13607*, 2020.
- [18] Jiezhong Qiu, Qibin Chen, Yuxiao Dong, Jing Zhang, Hongxia Yang, Ming Ding, Kuansan Wang, and Jie Tang. Gcc: Graph contrastive coding for graph neural network pre-training. In *Proceedings of the 26th ACM SIGKDD International Conference on Knowledge Discovery & Data Mining*, pages 1150–1160, 2020.
- [19] Zhanxuan Hu, Feiping Nie, Wei Chang, Shuzheng Hao, Rong Wang, and Xuelong Li. Multi-view spectral clustering via sparse graph learning. *Neurocomputing*, 384:1–10, 2020.
- [20] Sheng Li, Hongfu Liu, Zhiqiang Tao, and Yun Fu. Multi-view graph learning with adaptive label propagation. In *2017 IEEE International Conference on Big Data (Big Data)*, pages 110–115. IEEE, 2017.
- [21] Nikolas Adaloglou, Nicholas Vretos, and Petros Daras. Multi-view adaptive graph convolutions for graph classification. In *European Conference on Computer Vision*, pages 398–414. Springer, 2020.
- [22] Jiafeng Cheng, Qianqian Wang, Zhiqiang Tao, Deyan Xie, and Quanxue Gao. Multi-view attribute graph convolution networks for clustering. In *Proceedings of the Twenty-Ninth International Joint Conference on Artificial Intelligence. IJCAI*, 2020.
- [23] Xu Geng, Yaguang Li, Leye Wang, Lingyu Zhang, Qiang Yang, Jieping Ye, and Yan Liu. Spatiotemporal multi-graph convolution network for ride-hailing demand forecasting. In *Proceedings of the AAAI conference on artificial intelligence*, pages 3656–3663, 2019.
- [24] Xiao Wang, Meiqi Zhu, Deyu Bo, Peng Cui, Chuan Shi, and Jian Pei. Am-gcn: Adaptive multi-channel graph convolutional networks. In *Proceedings of the 26th ACM SIGKDD International Conference on Knowledge Discovery & Data Mining*, pages 1243–1253, 2020.
- [25] Lynn Margulis. Symbiosis and evolution. *Scientific American*, 225(2):48–61, 1971.
- [26] Daniel I Bolnick, Rowan DH Barrett, Krista B Oke, Diana J Rennison, and Yoel E Stuart. Annual review of ecology, evolution, and systematics. *Annu. Rev. Ecol. Evol. Syst.*, 49:303–30, 2018.
- [27] Sally E Smith and David J Read. *Mycorrhizal symbiosis*. Academic press, 2010.
- [28] Phuc H Le-Khac, Graham Healy, and Alan F Smeaton. Contrastive representation learning: A framework and review. *IEEE Access*, 2020.
- [29] Jiezhong Qiu, Yuxiao Dong, Hao Ma, Jian Li, Kuansan Wang, and Jie Tang. Network embedding as matrix factorization: Unifying deepwalk, line, pte, and node2vec. In *Proceedings of the eleventh ACM international conference on web search and data mining*, pages 459–467, 2018.
- [30] Fanxu Meng, Hao Cheng, Ke Li, Zhixin Xu, Rongrong Ji, Xing Sun, and Guangming Lu. Filter grafting for deep neural networks. In *Proceedings of the IEEE/CVF Conference on Computer Vision and Pattern Recognition*, pages 6599–6607, 2020.
- [31] Ravid Shwartz-Ziv and Naftali Tishby. Opening the black box of deep neural networks via information. *arXiv preprint arXiv:1703.00810*, 2017.
- [32] Hao Cheng, Dongze Lian, Shenghua Gao, and Yanlin Geng. Utilizing information bottleneck to evaluate the capability of deep neural networks for image classification. *Entropy*, 21(5):456, 2019.

- [33] Thomas N Kipf and Max Welling. Semi-supervised classification with graph convolutional networks. In *Proceedings of the International Conference on Learning Representations (ICLR)*, 2016.
- [34] Petar Veličković, Guillem Cucurull, Arantxa Casanova, Adriana Romero, Pietro Lio, and Yoshua Bengio. Graph attention networks. In *Proceedings of the International Conference on Learning Representations (ICLR)*, 2017.
- [35] William L Hamilton, Rex Ying, and Jure Leskovec. Inductive representation learning on large graphs. In *Advances in neural information processing systems*, pages 1024–1034, 2017.
- [36] Johannes Klicpera, Aleksandar Bojchevski, and Stephan Günnemann. Predict then propagate: Graph neural networks meet personalized pagerank. In *Proceedings of the International Conference on Learning Representations (ICLR)*, 2019.
- [37] Hongyang Gao and Shuiwang Ji. Graph u-nets. In *international conference on machine learning*, pages 2083–2092. PMLR, 2019.
- [38] Sami Abu-El-Haija, Bryan Perozzi, Amol Kapoor, Nazanin Alipourfard, Kristina Lerman, Hrayr Harutyunyan, Greg Ver Steeg, and Aram Galstyan. Mixhop: Higher-order graph convolutional architectures via sparsified neighborhood mixing. In *international conference on machine learning*, pages 21–29. PMLR, 2019.
- [39] Felix Wu, Amauri Souza, Tianyi Zhang, Christopher Fifty, Tao Yu, and Kilian Weinberger. Simplifying graph convolutional networks. In *International conference on machine learning*, pages 6861–6871. PMLR, 2019.
- [40] Vikas Verma, Meng Qu, Alex Lamb, Yoshua Bengio, Juho Kannala, and Jian Tang. Graphmix: Regularized training of graph neural networks for semi-supervised learning. *arXiv preprint arXiv:1909.11715*, 2019.
- [41] Ming Chen, Zhewei Wei, Zengfeng Huang, Bolin Ding, and Yaliang Li. Simple and deep graph convolutional networks. In *International Conference on Machine Learning*, pages 1725–1735. PMLR, 2020.
- [42] Prithviraj Sen, Galileo Namata, Mustafa Bilgic, Lise Getoor, Brian Galligher, and Tina Eliassi-Rad. Collective classification in network data. *AI magazine*, 29(3):93–93, 2008.
- [43] Galileo Namata, Ben London, Lise Getoor, Bert Huang, and UMD EDU. Query-driven active surveying for collective classification. In *10th International Workshop on Mining and Learning with Graphs*, volume 8, 2012.
- [44] Zhilin Yang, William Cohen, and Ruslan Salakhudinov. Revisiting semi-supervised learning with graph embeddings. In *International conference on machine learning*, pages 40–48. PMLR, 2016.
- [45] Benedek Rozemberczki, Carl Allen, and Rik Sarkar. Multi-scale attributed node embedding. *Journal of Complex Networks*, 9(2):cnab014, 2021.
- [46] Jie Tang, Jimeng Sun, Chi Wang, and Zi Yang. Social influence analysis in large-scale networks. In *Proceedings of the 15th ACM SIGKDD international conference on Knowledge discovery and data mining*, pages 807–816, 2009.
- [47] Hongbin Pei, Bingzhe Wei, Kevin Chen-Chuan Chang, Yu Lei, and Bo Yang. Geom-gcn: Geometric graph convolutional networks. In *Proceedings of the International Conference on Learning Representations (ICLR)*, 2020.
- [48] Christopher Morris, Nils M. Kriege, Franka Bause, Kristian Kersting, Petra Mutzel, and Marion Neumann. Tudataset: A collection of benchmark datasets for learning with graphs. In *ICML 2020 Workshop on Graph Representation Learning and Beyond (GRL+ 2020)*, 2020. URL www.graphlearning.io.
- [49] Weihua Hu, Matthias Fey, Marinka Zitnik, Yuxiao Dong, Hongyu Ren, Bowen Liu, Michele Catasta, and Jure Leskovec. Open graph benchmark: Datasets for machine learning on graphs. In *Advances in neural information processing systems*, 2020.

- [50] Kaili Ma, Haochen Yang, Han Yang, Tatiana Jin, Pengfei Chen, Yongqiang Chen, Barakeel Fansu Kamhoua, and James Cheng. Improving graph representation learning by contrastive regularization. *arXiv preprint arXiv:2101.11525*, 2021.
- [51] Federico Errica, Marco Podda, Davide Bacciu, and Alessio Micheli. A fair comparison of graph neural networks for graph classification. In *Proceedings of the International Conference on Learning Representations (ICLR)*, 2020.
- [52] Keyulu Xu, Chengtao Li, Yonglong Tian, Tomohiro Sonobe, Ken-ichi Kawarabayashi, and Stefanie Jegelka. Representation learning on graphs with jumping knowledge networks. In *International Conference on Machine Learning*, pages 5453–5462. PMLR, 2018.
- [53] Keyulu Xu, Weihua Hu, Jure Leskovec, and Stefanie Jegelka. How powerful are graph neural networks? In *Proceedings of the International Conference on Learning Representations (ICLR)*, 2019.
- [54] Lingxiao Zhao and Leman Akoglu. Pairnorm: Tackling oversmoothing in gnns. In *Proceedings of the International Conference on Learning Representations (ICLR)*, 2020.
- [55] Deli Chen, Yankai Lin, Wei Li, Peng Li, Jie Zhou, and Xu Sun. Measuring and relieving the over-smoothing problem for graph neural networks from the topological view. In *Proceedings of the AAAI Conference on Artificial Intelligence*, pages 3438–3445, 2020.
- [56] Meng Liu, Hongyang Gao, and Shuiwang Ji. Towards deeper graph neural networks. In *Proceedings of the 26th ACM SIGKDD International Conference on Knowledge Discovery & Data Mining*, pages 338–348, 2020.
- [57] Lutz Prechelt. Early stopping-but when? In *Neural Networks: Tricks of the trade*, pages 55–69. Springer, 1998.

A Algorithm

The pseudo-code of the GraphSym with multiple generated graph views is outlined in Algorithm 2. The training process involves generating multiple graph views, the individual phase, and the symbiotic phase. At the beginning (Line 1-2), we generate multiple graph views via the graph augmentations. Then, in the individual phase (Line 4-6), we train GNNs with the default hyper-parameter settings and update the weights of GNNs. At last, in the symbiotic phase (Line 10-15), we utilize the entropy criterion to decide what is valuable information to exchange and propose an adaptively exchange strategy to exchange redundant channels of one GNN (target network) with informative channels of another GNN (source network). Finally, we reverse the source and target network and repeat the above process (Line 16).

Algorithm 2: Graph symbiosis learning with multiple GNNs

Input: The original graph \mathcal{G} ; number of multiple graph views K , \mathcal{G}_k denotes the k -th generated graph view; GNN \mathcal{F}_k , whose input is \mathcal{G}_k ;
 $\theta_k^l = [\theta_k^{l,1}, \dots, \theta_k^{l,C_{l+1}}] \in \mathbb{R}^{C_l \times C_{l+1}}$ denotes the weight in the l -th layer of a GNN corresponding to the k -th generated graph view, whose input channel is C_l and output channel is C_{l+1} and $\theta_k^{l,j} \in \mathbb{R}^{C_l}$ is the vector of the j -th channel; the number layers of \mathcal{F}_k is L ; learning rate η ; iteration number N ; number of exchange channels M ; the graph augmentation functions \mathcal{C} to get multiple graph views.

Output: Prediction \mathbf{Z}

- 1 **for** $k = 1 : K$ **do**
- 2 Get the graph view \mathcal{G}_k via the graph augmentation function $\mathcal{G}_k = \mathcal{C}(\mathcal{G})$.
- 3 **▷ The individual phase:**
- 4 **for** $k = 1 : K$ **do**
- 5 Train GNN $\mathcal{F}_k(\mathcal{G}_k; \theta_k)$ and compute the supervised classification loss \mathcal{L} .
- 6 Update the weight θ_k by gradient descent: $\theta_k = \theta_k - \eta \nabla_{\theta} \mathcal{L}$.
- 7 **▷ The symbiotic phase:**
- 8 **for** $n = 1 : N$ **do**
- 9 **for** $k = 1 : K$ **do**
- 10 Get the source and target GNN: $s, t = k, (k + 1) \% K$.
- 11 **for** $l = 1 : L$ **do**
- 12 Calculate the Pearson correlations among all possible pairs of the channels in θ_t^l .
- 13 Find a pair of channels indexed by idx_1 and idx_2 with the highest correlation.
- 14 **for** $m = 1 : M$ **do**
- 15 Substitute each channel of the source network θ_s^l for $\theta_t^{l,\text{idx}_1}$ or $\theta_t^{l,\text{idx}_2}$ of the target network to find an informative channel as Eq. 3.
- 16 **for** $k = K : 1$ **do**
- 17 Exchange the role of the source and target networks: $s, t = (k + 1) \% K, k$.
- 18 Repeat line 11-15.
- 19 **Output** prediction \mathbf{Z} via re-training $\mathbf{Z} = \mathcal{F}_1(\mathcal{G}; \theta_1)$.

B Graph augmentations

We implement the commonly-used graph augmentation methods in previous work to generate multiple graph views [9, 13, 10].

- *Masking node features.* Randomly mask a fraction of node attributes with zeros. Formally, the generated node features matrix $\widetilde{\mathbf{X}}$ is computed by

$$\widetilde{\mathbf{X}} = [\mathbf{x}_1 \odot \mathbf{m}, \mathbf{x}_2 \odot \mathbf{m}, \dots, \mathbf{x}_N \odot \mathbf{m}], \quad (4)$$

where $\mathbf{m} \in \{0, 1\}^d$ is a random vector, which is drawn from a Bernoulli distribution, $[\cdot; \cdot]$ is the concatenation operator, and \odot is the element-wise multiplication.

- *Corrupting node features.* Randomly replace a fraction of node attributes with Gaussian noise. Formally, it can be calculated as follows,

$$\widetilde{\mathbf{X}} = [\mathbf{x}_1 \odot \mathbf{m}_1, \mathbf{x}_2 \odot \mathbf{m}_2, \dots, \mathbf{x}_N \odot \mathbf{m}_n], \quad (5)$$

where $\mathbf{m}_i \in \mathbb{R}^d$ is a random vector drawn from a Gaussian distribution $\mathcal{N}(\mu(\mathbf{x}_i), 1)$ independently and $\mu(\cdot)$ is the mean value of a vector.

- *Dropping edges.* Randomly remove edges in the graph. Formally, we sample a modified subset $\widetilde{\mathcal{E}}$ from the original edge set \mathcal{E} with probability defined as follows:

$$P\{(u, v) \in \widetilde{\mathcal{E}}\} = 1 - p_{uv}^e, \quad (6)$$

where $(u, v) \in \mathcal{E}$ and p_{uv}^e is the probability of removing (u, v) .

- *Extracting subgraphs.* Extract the induced subgraphs $\mathcal{G}' = (\mathcal{V}', \mathcal{E}')$ containing the nodes in a given subset, *i.e.*, $\mathcal{V}' \subseteq \mathcal{V}$ and $\mathcal{E}' \subseteq \mathcal{E}$, which follows the experimental setting in [13].

C Preliminaries of GNNs

Graph neural networks. The training process of modern GNNs follow the message-passing mechanism [3]. During each message-passing iteration, a hidden embedding $\mathbf{h}_u^{(k)}$ corresponding to each node $u \in \mathcal{V}$ is updated by aggregating information from u 's neighborhood $\mathcal{N}(u)$, which can be expressed as follows:

$$\begin{aligned} \mathbf{h}_u^{(k+1)} &= \text{UPDATE}^{(k)} \left(\mathbf{h}_u^{(k)}, \text{AGGREGATE}^{(k)} \left(\left\{ \mathbf{h}_v^{(k)}, \forall v \in \mathcal{N}(u) \right\} \right) \right) \\ &= \text{UPDATE}^{(k)} \left(\mathbf{h}_u^{(k)}, \mathbf{m}_{\mathcal{N}(u)}^{(k)} \right), \end{aligned} \quad (7)$$

where UPDATE and AGGREGATE are arbitrary differentiable functions (*i.e.*, neural networks), and $\mathbf{m}_{\mathcal{N}(u)}$ denotes the ‘‘message’’ that is aggregated from u 's neighborhood $\mathcal{N}(u)$. The initial embedding at $k = 0$ is set to the input features, *i.e.*, $\mathbf{h}_u^{(0)} = \mathbf{x}_u, \forall u \in \mathcal{V}$. After running k iterations of the GNN message-passing, we can obtain information from k -hops neighborhood nodes. Different GNNs can be obtained by choosing different UPDATE and AGGREGATE functions. For example, the classical Graph Convolutional Networks (GCN) [33] updates the hidden embedding as

$$\mathbf{H}^{(l+1)} = \sigma \left(\hat{\mathbf{A}} \mathbf{H}^{(l)} \mathbf{W}^{(l)} \right), \quad (8)$$

where $\mathbf{H}^{(l+1)} = [\mathbf{h}_1^{(l+1)}; \dots; \mathbf{h}_n^{(l+1)}]$ is the hidden matrix of the $(l+1)$ -th layer. $\hat{\mathbf{A}} = \hat{\mathbf{D}}^{-1/2}(\mathbf{A} + \mathbf{I})\hat{\mathbf{D}}^{-1/2}$ is the re-normalization of the adjacency matrix, and $\hat{\mathbf{D}}$ is the corresponding degree matrix of $\mathbf{A} + \mathbf{I}$. $\mathbf{W}^{(l)} \in \mathbb{R}^{C_l \times C_{l+1}}$ is the filter matrix in the l -th layer with C_l referring to the size of l -th hidden layer and $\sigma(\cdot)$ is a nonlinear function, *e.g.* ReLU.

Problem setup. In this work, we focus on undirected and unweighted graphs. However, it is straightforward to extend this work to directed and weighted graphs. Let $\mathcal{G} = (\mathcal{V}, \mathcal{E}, \mathbf{X})$ denote a graph, where \mathcal{V} is the a set of $|\mathcal{V}| = n$ nodes, \mathcal{E} is a set of $|\mathcal{E}| = m$ edges between nodes, $\mathbf{X} = [\mathbf{x}_1, \mathbf{x}_2, \dots, \mathbf{x}_N]^T \in \mathbb{R}^{n \times d}$ represents the node feature matrix and $\mathbf{x}_i \in \mathbb{R}^d$ is the feature vector of node v_i . The adjacency matrix $\mathbf{A} \in \{0, 1\}^{n \times n} \subseteq \mathcal{V} \times \mathcal{V}$ is defined by $\mathbf{A}_{i,j} = 1$ *iff* $(v_i, v_j) \in \mathcal{E}$, otherwise $\mathbf{A}_{i,j} = 0$. Following the common semi-supervised transductive node classification setting, only a small part of nodes $\mathcal{V}_{\text{train}} = \{v_1, v_2, \dots, v_l\}$ are given, whose corresponding labels are $\mathcal{Y}_{\text{train}} = \{y_1, y_2, \dots, y_l\}$, where y_i is the label of v_i . Our goal is to use this partial information to infer the missing labels for nodes $\mathcal{V} \setminus \mathcal{V}_{\text{train}}$. Similarly, for the link prediction task, we are given the node set \mathcal{V} and an incomplete set of edges between these nodes $\mathcal{E}_{\text{train}} \subset \mathcal{E}$, and our goal is to infer the missing edges $\mathcal{E} \setminus \mathcal{E}_{\text{train}}$. For graph classification problems, given a set of graphs $\{\mathcal{G}_1, \mathcal{G}_2, \dots, \mathcal{G}_N\} \subseteq \mathbb{G}$ and their labels $\{l_1, l_2, \dots, l_N\} \subseteq \mathbb{L}$, our goal is to learn a function $f : \mathbb{G} \rightarrow \mathbb{L}$ and predict the label of other graphs.

Table 6: Statistics of the real-world datasets.

	# Nodes: $ \mathcal{V} $	# Edges: $ \mathcal{E} $	# Features: \mathbf{d}	# classes: $ \mathcal{Y} $
Cora	2,708	5,278	1,433	7
CiteSeer	3,327	4,676	3,703	6
PubMed	19,717	44,327	500	3
Chameleon	2,277	31,421	2,325	5
Squirrel	5,201	198,493	2,089	5
Actor	7,600	26,752	931	5
Cornell	183	280	1,703	5
Texas	183	295	1,703	5
Wisconsin	251	466	1,703	5
ogbn-arxiv	169,343	1,166,243	128	40
	# Graphs: $ \mathcal{G} $	# Average nodes: $ \mathcal{V} / \mathcal{G} $	# Average edges: $ \mathcal{E} / \mathcal{G} $	# classes: $ \mathcal{L} $
DD	1,178	284.32	715.66	2
NCI1	4,110	29.87	32.30	2
PROTEINS	1,113	39.06	72.82	2
IMDB-BINARY	1,000	19.77	96.52	2
REDDIT-BINARY	2,000	429.63	497.75	2

Training targets and loss functions. Here we briefly summarize the training targets of the node classification, link prediction and graph classification. We denote node and edge embedding of the final layer of a GNN as \mathbf{z}_u and $\mathbf{z}_{(u,v)}$, and graph-level embedding performed by a readout functions as \mathbf{z}_G . Then GNNs can be trained in an end-to-end manner using the following loss function:

$$\begin{aligned} \mathcal{L}_{\text{node}} &= \frac{1}{|\mathcal{V}_{\text{train}}|} \sum_{u \in \mathcal{V}_{\text{train}}} \text{Loss}(\mathbf{z}_u, \mathbf{y}_u); \mathcal{L}_{\text{edge}} = \frac{1}{|\mathcal{E}_{\text{train}}|} \sum_{(u,v) \in \mathcal{E}_{\text{train}}} \text{Loss}(\mathbf{z}_{(u,v)}, \mathbf{y}_{(u,v)}); \\ \mathcal{L}_{\text{graph}} &= \frac{1}{|\mathcal{G}|} \sum_{G_i \in \mathcal{G}} \text{Loss}(\mathbf{z}_{G_i}, \mathbf{y}_{G_i}), \end{aligned} \quad (9)$$

where \mathbf{y}_u , $\mathbf{y}_{(u,v)}$ and \mathbf{y}_{G_i} are the true labels of the corresponding node, edge and graph, respectively. For example, *Loss* can be the cross-entropy loss in the node/graph classification task or the 0/1 loss in the edge prediction problem.

D Datasets

In this section, we describe the details (including nodes, edges, features, and classes for node/edge datasets and graphs, average nodes, average edges, and classes for graph datasets) of the real-world graph datasets used in this paper. We report the statistics of these real-world datasets in Table 6. The descriptions of each of these datasets and their data splits are given as follows:

- **Cora, CiteSeer, and PubMed** are academical citation networks originally introduced in [42–44], which are the most widely used benchmark datasets for semi-supervised node classification [44]. In these networks, nodes represent papers and edges denote the citation of one paper by another. Node features are the bag-of-words representation for each node and node label is the academic topic of a paper. We follow the public fixed split from the [44]. We use 20 samples per class for the training, 500 samples for the validation, and 1000 samples for the test.
- **Chameleon and Squirrel** are two page-page graphs on specific topics in Wikipedia network [45]. In these datasets, nodes represent the web pages and edges denote mutual links between pages. Node features are several informative nouns in the Wikipedia pages. We follow the node labels generated by [47], where nodes are classified into five categories in term of the number of the average monthly traffic of the web page. Following the method in [47], we randomly split nodes of each class into 60%, 20%, and 20% for training, validation and testing.
- **Actor** is the actor co-occurrence induced subgraph of the film-director-actor-writer network [46]. In this network, nodes represent actors and the edge between two nodes denotes the co-occurrence

on the same Wikipedia page. Node features are generated by some keywords in the Wikipedia pages. Following the node labels generated by [47], we classify the nodes into five categories in term of words of corresponding actor’s Wikipedia. Following the method in [47], we randomly split nodes of each class into 60%, 20%, and 20% for training, validation and testing.

- **Cornell, Texas, and Wisconsin** are webpage datasets of computer departments in universities, *i.e.*, Cornell, Texas, and Wisconsin. In these datasets, nodes represent web pages and edges denote the hyperlinks between them. Node features are the bag-of-words representation of corresponding web pages. We also follow the node labels generated by [47], where nodes are classified into five categories according to the identity of people. Following the method in [47], we randomly split nodes of each class into 60%, 20%, and 20% for training, validation and testing.
- **Ogbn-arxiv** is a recently proposed large-scale dataset of paper citation networks [49]. Nodes represent arXiv papers and edges denote the citations between two papers. Node features are 128-dimensional feature vectors obtained by averaging the embeddings of words in its title and abstract and node labels are the primary categories of the arXiv papers. We use the public data split based on the publication dates of the papers.
- **DD, NCI1, and PROTEINS** are chemical compound datasets introduced in [48]. The nodes represent secondary structure elements (SSEs) and edges between two nodes denote neighborhood relationship in the amino-acid sequence or in 3D space. We use one-hot embedding vector to denote features of different nodes. Node labels are categorised into two classes according to its chemical property. Following the method in [51], we randomly split nodes of each class into 80%, 10%, and 10% for training, validation and testing.
- **IMDB-BINARY, REDDIT-BINARY** are social networks, representing movie collaboration and online discuss forum, respectively. Nodes represent actors/actresses and users, respectively. Edges between two nodes denote they appear in the same movie in IMDB-BINARY and one user respond to another’s comment in REDDIT-BINARY. We use one-hot embedding vector to denote features of different nodes. Node labels are categorised into two classes according to their community or subreddit. Following the method in [51], we randomly split nodes of each class into 80%, 10%, and 10% for training, validation and testing.

E The Experimental Setup

For the reproducibility, we provide our experimental environment, baseline GNN models, datasets websites and implementation details. The implementation details include the experimental settings, detailed hyper-parameters in their original papers that we follow, and the configurations of graph augmentation methods.

E.1 Experiments Settings

All experiments are conducted with the following settings:

- Operating system: Ubuntu Linux 16.04.7 LTS
- CPU: Intel(R) Xeon(R) Silver 4210 CPU @ 2.20GHz
- GPU: NVIDIA GP102GL [Tesla P40]
- Software versions: Python 3.7; Pytorch 1.7.0; Numpy 1.16.2; SciPy 1.2.1; Pandas 1.0.5; scikit-learn 0.23.1; PyTorch-geometric 1.6.3; Open Graph Benchmark 1.3.1

E.2 Baseline GNNs and Datasets

We follow the experimental settings in their original paper. Table 7 summarizes URLs and commit numbers of baseline codes. Datasets used in this paper can be found in the following URLs, shown in Table 8.

E.3 Implementation Details

The codes of GraphSym in Table 1 in the main body are based on GRAND [10] codebase. All implementation of codes can be found in the supplementary materials. For the reproducibility

Table 7: Baseline GNNs.

	Methods	URL	Commit
Node classification	GCN	https://github.com/rusty1s/pytorch_geometric	db3bdc2
	GAT	https://github.com/rusty1s/pytorch_geometric	db3bdc2
	APPNP	https://github.com/benedekroczemberczki/APPNP	fce0d76
	JKNET-CAT	https://github.com/rusty1s/pytorch_geometric	db3bdc2
	JKNET-MAX	https://github.com/rusty1s/pytorch_geometric	db3bdc2
	GCNII	https://github.com/chennnM/GCNII	ca91f56
	GRAND	https://github.com/THUDM/GRAND	ba164c6
Edge prediction	GCN-EDGE	https://github.com/rusty1s/pytorch_geometric	e6b8d6
Graph classification	GCN-GRAPH	https://github.com/diningphil/gnn-comparison	0e0e9b1
	GIN	https://github.com/rusty1s/pytorch_geometric	db3bdc2
ogbn-arxiv	GCN-RES-v2	https://github.com/ytchx1999/GCN_res-CS-v2	a3e7d1f
	GCN-DGL	https://github.com/Espylapiza/dgl	5feada0
	GraphSAGE	https://github.com/snap-stanford/ogb	be38132

Table 8: Datasets.

Datasets	URL
Cora, CiteSeer, PubMed	https://github.com/rusty1s/pytorch_geometric
Chameleon, Squirrel	https://github.com/graphdml-uiuc-jlu/geom-gcn
Actor	https://github.com/graphdml-uiuc-jlu/geom-gcn
Cornell, Texas, Wisconsin	https://github.com/graphdml-uiuc-jlu/geom-gcn
DD, NCI1, PROTEINS	https://github.com/rusty1s/pytorch_geometric
IMDB-BINARY, REDDIT-BINARY	https://github.com/rusty1s/pytorch_geometric
ogbn-arxiv	https://github.com/snap-stanford/ogb

of our proposed framework, we also list all the hyper-parameter values used in our framework. *Tolerance_num* means number of epochs with no improvement after which training will be stopped. *Tolerance* denotes the quantity to be monitored in early stopping mechanism, which has three choices: *loss*, *accuracy*, and *both*. Specifically, *loss* means the training stops when the loss monitored metric has stopped decreasing, *accuracy* means the process stops when the accuracy monitored metric has stopped increasing, and *both* means the process stops when the loss monitored metric has stopped decreasing or the accuracy monitored metric has stopped increasing. The details are as follows.

- **GCN [33]:**

- All node classification datasets: layers: 2; hidden: 16; dropout: 0.5; epochs: 200; lr: 0.01; tolerance: loss; tolerance_num: 10; weight_decay: 5e-4 in the first GCN and 0 in the second GCN.

- **GAT [34]:**

- All node classification datasets except PubMed: layers: 2; hidden: 8; heads: 8; dropout: 0.6; attention_drop:0.6; epochs: 100000; lr: 0.005; tolerance: both; tolerance_num: 100; weight_decay: 0.0005.
- PubMed: layers: 2; hidden: 8; heads: 8; dropout: 0.6; attention_drop:0.6; epochs: 100000; lr: 0.01; tolerance: both; tolerance_num: 100; weight_decay: 0.001.

- **APPNP [36]:**

- All node classification datasets: layers: 2; hidden: 64; dropout: 0.5; epochs: 2000; lr: 0.01; tolerance: accuracy; tolerance_num: 500; weight_decay: 0.

- **JKNET-CAT [52]:**

- All node classification datasets: layers: 2; hidden: 32; dropout: 0.75; epochs: 1500; lr: 0.005; tolerance: loss; tolerance_num: 100; weight_decay: 0.0005; mode: cat.

- **JKNET-MAX [52]:**

- All node classification datasets: layers: 2; hidden: 32; dropout: 0.75; epochs: 1500; lr: 0.005; tolerance: loss; tolerance_num: 100; weight_decay: 0.0005; mode: max.

- **GCNII [41]:**
 - Cora: layers: 64; hidden: 64; dropout: 0.6; epochs: 1500; lr: 0.01; tolerance: loss; tolerance_num: 100; weight_decay: 0.01 for dense layer and 0.0005 for convolutional layer; λ : 0.5; α : 0.1.
 - CiteSeer: layers: 32; hidden: 256; dropout: 0.7; epochs: 1500; lr: 0.01; tolerance: loss; tolerance_num: 100; weight_decay: 0.01 for dense layer and 0.0005 for convolutional layer; λ : 0.6; α : 0.1.
 - PubMed: layers: 16; hidden: 256; dropout: 0.5; epochs: 1500; lr: 0.01; tolerance: loss; tolerance_num: 100; weight_decay: 0.0005 for dense layer and 0.0005 for convolutional layer; λ : 0.4; α : 0.1.
 - Chameleon, Squirrel, Actor: layers: 8; hidden: 64; dropout: 0.5; epochs: 1500; lr: 0.01; tolerance: loss; tolerance_num: 100; weight_decay: 0.0005; λ : 1.5; α : 0.2.
 - Cornell: layers: 16; hidden: 64; dropout: 0.5; epochs: 1500; lr: 0.01; tolerance: loss; tolerance_num: 100; weight_decay: 0.001; λ : 1; α : 0.5.
 - Texas: layers: 32; hidden: 64; dropout: 0.5; epochs: 1500; lr: 0.01; tolerance: loss; tolerance_num: 100; weight_decay: 0.0001; λ : 1.5; α : 0.5.
 - Wisconsin: layers: 16; hidden: 64; dropout: 0.5; epochs: 1500; lr: 0.01; tolerance: loss; tolerance_num: 100; weight_decay: 0.0005; λ : 1; α : 0.5.
 - ogbn-arxiv: layers: 16; hidden: 256; dropout: 0.1; epochs: 1000; lr: 0.001; tolerance: accuracy; tolerance_num: 200; weight_decay: 0; λ : 1; α : 0.5.
- **GRAND [10]:**
 - Cora: layers: 2; hidden: 32; input_dropout: 0.5; hidden_dropout: 0.5; epochs: 5000; lr: 0.01; tolerance: both; tolerance_num: 200; weight_decay: 0.0005; droptnode_rate 0.5; lambda: 1.0; temperature: 0.5; order: 8; sample: 4.
 - CiteSeer: layers: 2; hidden: 32; input_dropout: 0.0; hidden_dropout: 0.2; epochs: 5000; lr: 0.01; tolerance: both; tolerance_num: 200; weight_decay: 0.0005; droptnode_rate 0.5; lambda: 0.7; temperature: 0.3; order: 2; sample: 2.
 - PubMed: layers: 2; hidden: 32; input_dropout: 0.6; hidden_dropout: 0.8; epochs: 5000; lr: 0.01; tolerance: both; tolerance_num: 200; weight_decay: 0.0005; droptnode_rate 0.5; lambda: 1.0; temperature: 0.2; order: 5; sample: 4; use_batchnorm: True.
- **GCN-EDGE³**
 - All edge prediction datasets: layers: 2; hidden: 128; dropout: 0.5; epochs: 100; lr: 0.01; weight_decay: 0.
- **GCN-GRAPH [51]:**
 - All graph classification datasets: batch: 50; layers: 2; hidden: 32; dense: 128; dropout: 0.5; epochs: 1000; lr: 0.0001; weight_decay: 0; k: 0.9.
- **GIN [53]:**
 - All graph classification datasets: batch: 32; layers: 5; hidden: 64; dropout: 0.5; epochs: 1000; lr: 0.01; weight_decay: 0; opt_scheduler: step.
- **GCN-RES-v2⁴:**
 - ogbn-arxiv: layers: 8; hidden: 128; dropout: 0.5; epochs: 500; lr: 0.01; weight_decay: 0.
- **GCN-DGL⁵:**
 - ogbn-arxiv: layers: 3; hidden: 256; dropout: 0.75; epochs: 1000; lr: 0.005; weight_decay: 0.
- **GraphSAGE⁶:**
 - ogbn-arxiv: layers: 5; hidden: 1024; dropout: 0.5; epochs: 100; lr: 0.001; weight_decay: 0.

³https://github.com/rusty1s/pytorch_geometric/blob/master/examples/link_pred.py

⁴https://github.com/ytchx1999/GCN_res-CS-v2

⁵<https://github.com/Espylapiza/dgl/blob/master/examples/pytorch/ogb/ogbn-arxiv/models.py>

⁶<https://github.com/snap-stanford/ogb/blob/master/examples/nodeproppred/ogbn-arxiv/gnn.py>

E.4 Configurations of the graph augmentation methods

In this section, we list the probability parameters controlling the sampling process in graph augmentations to generate multiple graph views of all experiments in the main body.

- **GCN [33]:**
 - Cora, CiteSeer, Cornell: masking node features: 0.1; Corrupting node features: 0.0; Dropping edges: 0.1; Extracting subgraphs: 0.0.
 - Other node classification datasets: masking node features: 0.1; Corrupting node features: 0.0; Dropping edges: 0.1; Extracting subgraphs: 0.1.
- **GAT [34]:**
 - PubMed, Squirrel, Actor: masking node features: 0.1; Corrupting node features: 0.0; Dropping edges: 0.1; Extracting subgraphs: 0.0.
 - Chameleon, Squirrel, Actor: masking node features: 0.4; Corrupting node features: 0.4; Dropping edges: 0.4; Extracting subgraphs: 0.4.
 - Cornell: masking node features: 0.1; Corrupting node features: 0.0; Dropping edges: 0.0; Extracting subgraphs: 0.0.
 - Other node classification datasets: masking node features: 0.1; Corrupting node features: 0.0; Dropping edges: 0.1; Extracting subgraphs: 0.1.
- **APPNP [36]:**
 - Chameleon: masking node features: 0.5; Corrupting node features: 0.5; Dropping edges: 0.5; Extracting subgraphs: 0.5.
 - Actor: masking node features: 0.0; Corrupting node features: 0.1; Dropping edges: 0.0; Extracting subgraphs: 0.0.
 - Cornell, Wisconsin: masking node features: 0.4; Corrupting node features: 0.4; Dropping edges: 0.4; Extracting subgraphs: 0.4.
 - Texas: masking node features: 0.6; Corrupting node features: 0.6; Dropping edges: 0.6; Extracting subgraphs: 0.6.
 - Other node classification datasets: masking node features: 0.1; Corrupting node features: 0.0; Dropping edges: 0.1; Extracting subgraphs: 0.1.
- **JKNET-CAT [52]:**
 - CiteSeer, Chameleon, Squirrel, Cornell: masking node features: 0.0; Corrupting node features: 0.0; Dropping edges: 0.1; Extracting subgraphs: 0.0.
 - PubMed: masking node features: 0.1; Corrupting node features: 0.0; Dropping edges: 0.1; Extracting subgraphs: 0.0.
 - Other node classification datasets: masking node features: 0.1; Corrupting node features: 0.0; Dropping edges: 0.1; Extracting subgraphs: 0.1.
- **JKNET-MAX [52]:**
 - CiteSeer, PubMed, Squirrel, Cornell: masking node features: 0.0; Corrupting node features: 0.0; Dropping edges: 0.1; Extracting subgraphs: 0.0.
 - Actor: masking node features: 0.2; Corrupting node features: 0.2; Dropping edges: 0.2; Extracting subgraphs: 0.2.
 - Texas: masking node features: 0.2; Corrupting node features: 0.1; Dropping edges: 0.1; Extracting subgraphs: 0.0.
 - Other node classification datasets: masking node features: 0.1; Corrupting node features: 0.0; Dropping edges: 0.1; Extracting subgraphs: 0.1.
- **GCNII [41]:**
 - Cornell: masking node features: 0.6; Corrupting node features: 0.6; Dropping edges: 0.6; Extracting subgraphs: 0.6.
 - Actor: masking node features: 0.3; Corrupting node features: 0.3; Dropping edges: 0.3; Extracting subgraphs: 0.3.
 - Texas, Wisconsin: masking node features: 0.2; Corrupting node features: 0.2; Dropping edges: 0.2; Extracting subgraphs: 0.2.

- Other node classification datasets: masking node features: 0.1; Corrupting node features: 0.0; Dropping edges: 0.1; Extracting subgraphs: 0.1.
- **GRAND [10]:**
 - All node classification datasets: masking node features: 0.1; Corrupting node features: 0.0; Dropping edges: 0.1; Extracting subgraphs: 0.1.
- **GCN-EDGE⁷**
 - All edge prediction datasets: masking node features: 0.1; Corrupting node features: 0.0; Dropping edges: 0.1; Extracting subgraphs: 0.1.
- **GCN-GRAPH [51]:**
 - All graph classification datasets: masking node features: 0.1; Corrupting node features: 0.0; Dropping edges: 0.1; Extracting subgraphs: 0.1.
- **GIN [53]:**
 - All graph classification datasets: masking node features: 0.1; Corrupting node features: 0.0; Dropping edges: 0.1; Extracting subgraphs: 0.1.
- **GCN-RES-v2⁸:**
 - ogbn-arxiv: masking node features: 0.1; Corrupting node features: 0.0; Dropping edges: 0.1; Extracting subgraphs: 0.1.
- **GCN-DGL⁹:**
 - ogbn-arxiv: masking node features: 0.1; Corrupting node features: 0.0; Dropping edges: 0.1; Extracting subgraphs: 0.1.
- **GraphSAGE¹⁰:**
 - ogbn-arxiv: masking node features: 0.1; Corrupting node features: 0.0; Dropping edges: 0.1; Extracting subgraphs: 0.1.

F Additional Experimental Results

In this section, we plot the training loss and accuracy curves as a sanity check to investigate whether GraphSym can train better than the original GNN baseline models. Figure 7 shows the accuracy curve and the loss curve of GraphSym and GCNII on ogbn-arxiv. The curve is recorded on the training set. We can observe that the blue line (GraphSym) is above the orange line (GCNII) in Figure 7(a), while the blue line (GraphSym) is under the orange line (GCNII) in Figure 7(b). We can empirically conclude that GraphSym can actually train better as a sanity check.

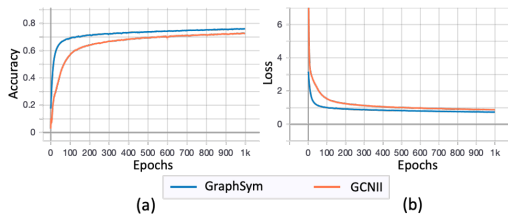


Figure 7: Accuracy and loss on ogbn-arxiv.

We also plot the accuracy and loss curves of GCN, GAT, APPNP, JKNET-CAT, JKNET-MAX, and GCN2 on Cora, CiteSeer, and PubMed datasets. Note that some lines in figures do not reach the end of training epochs because of the early stopping mechanism [57] used in the original paper. From Figure 8, we can find that the blue line (multi-view symbiosis) is always above the orange line (original GNN). From Figure 9, we can find that the blue line (multi-view symbiosis) is always under the orange line (original GNN). These figures indicate that GraphSym consistently outperforms the original GNN baseline models and suggest that GraphSym can empirically improve the training process of the original GNNs.

⁷https://github.com/rusty1s/pytorch_geometric/blob/master/examples/link_pred.py

⁸https://github.com/ytchx1999/GCN_res-CS-v2

⁹<https://github.com/Espylapiza/dgl/blob/master/examples/pytorch/ogb/ogbn-arxiv/models.py>

¹⁰<https://github.com/snap-stanford/ogb/blob/master/examples/nodeproppred/ogbn-arxiv/gnn.py>

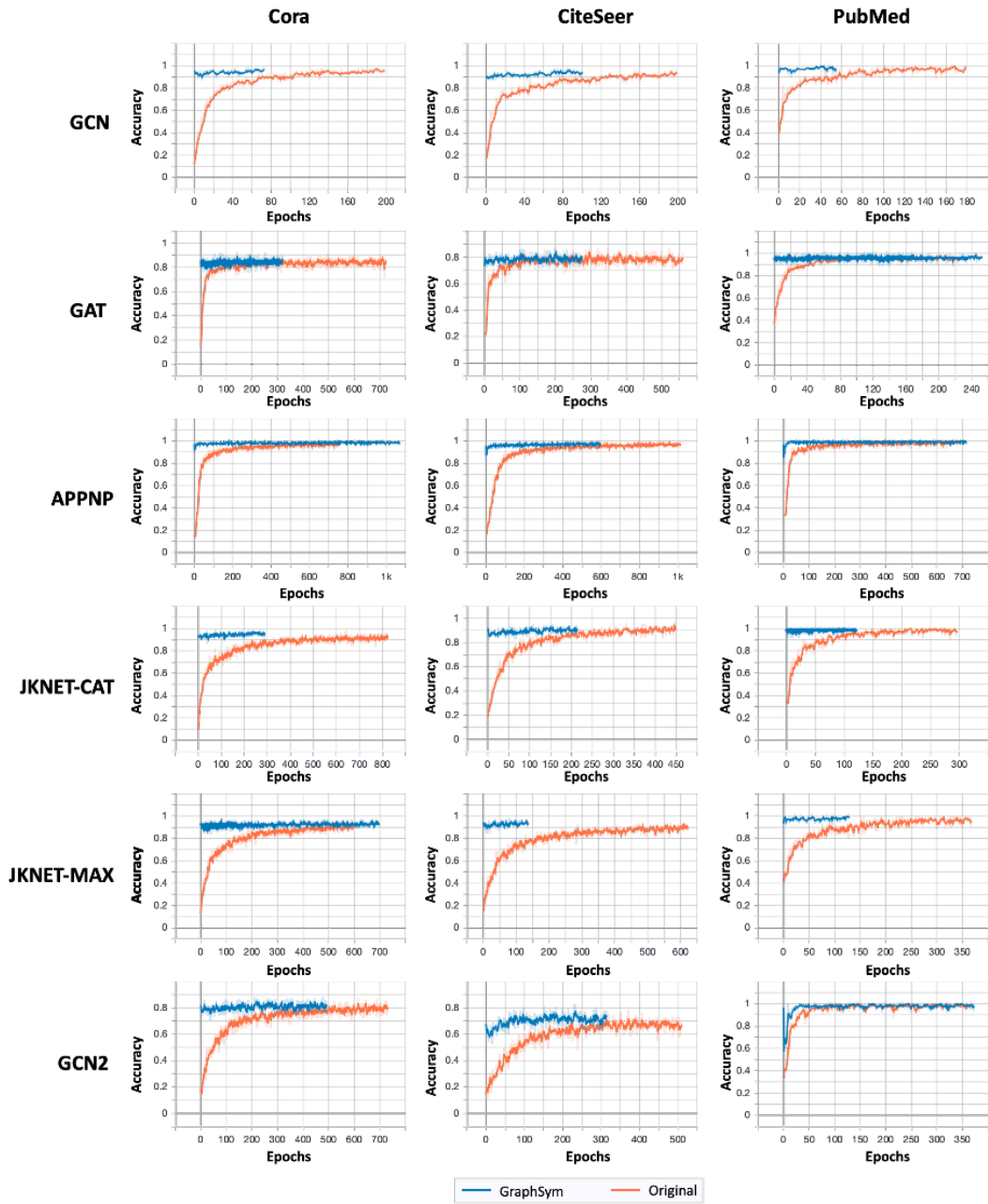


Figure 8: Accuracy curves on comparison between the baseline GNNs and GraphSym on Cora, CiteSeer, and PubMed.

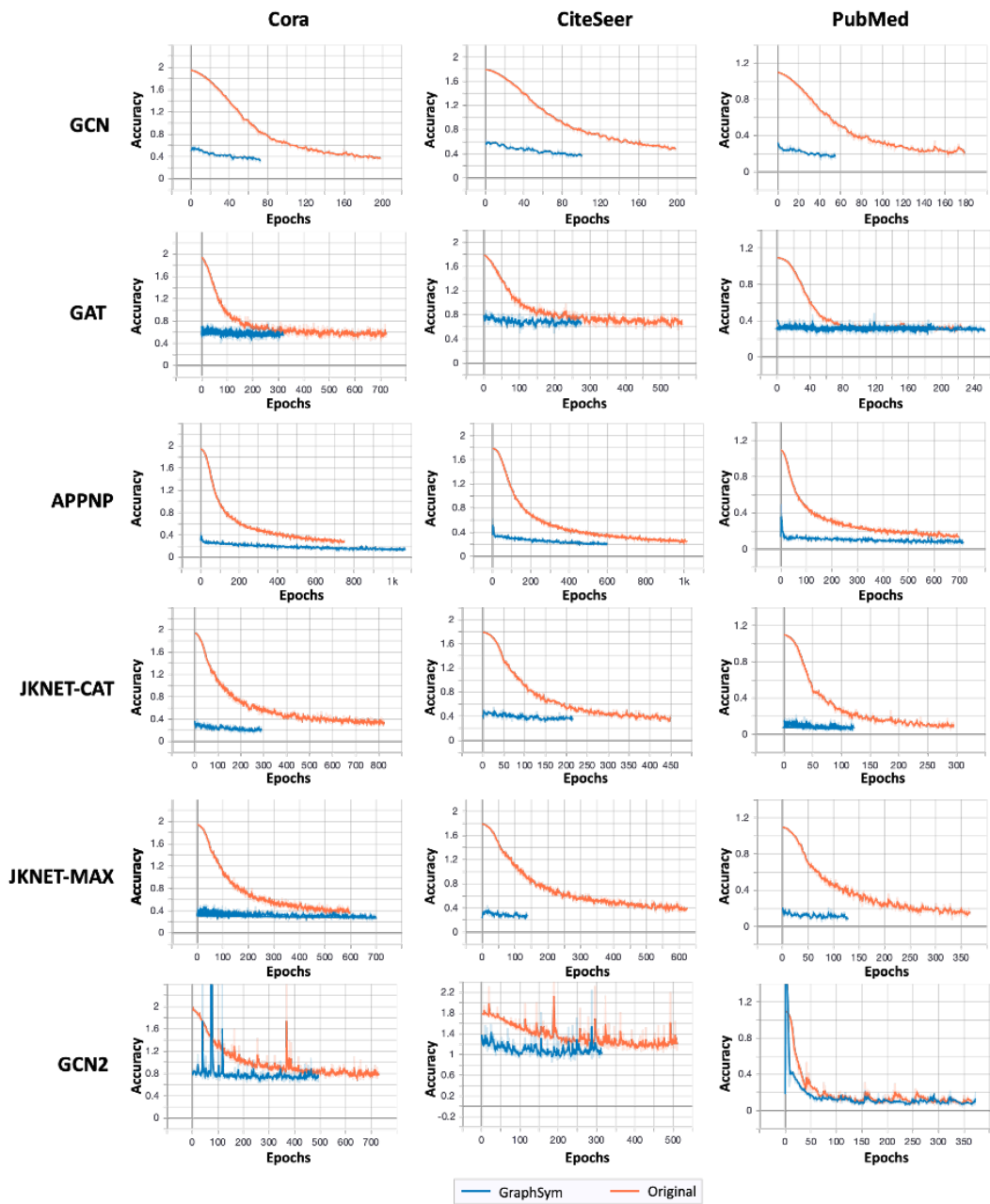


Figure 9: Loss curves on comparison between the baseline GNNs and GraphSym on Cora, CiteSeer, and PubMed.